

RESEARCH

Open Access



MAIT cell deficiency exacerbates neuroinflammation in P301S human tau transgenic mice

Yuanyue Zhang^{1†}, Zhi Yang^{1†}, Na Jiang^{1†}, Xiaosheng Tan¹, Peng Jiang³, Gaoyuan Cao² and Qi Yang^{1,2,4*}

Abstract

Background The role of immune cells in neurodegeneration remains incompletely understood. Accumulation of misfolded tau proteins is a hallmark of neurodegenerative diseases. Our recent study revealed the presence of mucosal-associated invariant T (MAIT) cells in the meninges, where they express antioxidant molecules to maintain meningeal barrier integrity. However, the role of MAIT cells in tau-related neuroinflammation and neurodegeneration remains unknown.

Methods Flow cytometry analysis was performed to examine MAIT cells in human Tau P301S transgenic mice. Tau pathology, hippocampus atrophy, meningeal integrity, and microglial gene expression were examined in *Mr1*^{-/-} P301S mice that lacked MAIT cells and control P301S transgenic mice, as well as *Mr1*^{-/-} P301S mice with adoptive transfer of MAIT cells.

Results The meninges of P301S mutant human tau transgenic mice had increased numbers of MAIT cells, which retained their expression of antioxidant molecules. *Mr1*^{-/-} P301S mice that lacked MAIT cells exhibited increased tau pathology and hippocampus atrophy compared to control *Mr1*^{+/+} P301S mice. Adoptive transfer of MAIT cells reduced tau pathology and hippocampus atrophy in *Mr1*^{-/-} P301S mice. Meningeal barrier integrity was compromised in *Mr1*^{-/-} P301S mice, but not in control *Mr1*^{+/+} P301S mice. A distinctive microglia subset with a proinflammatory gene expression profile (M-inflammatory) was enriched in the hippocampus of *Mr1*^{-/-} P301S mice. The transcriptomes of the remaining microglia in these mice also shifted towards a proinflammatory state, with increased expression of inflammatory cytokines, chemokines, and genes related to ribosome biogenesis and immune responses to toxic substances. The transfer of MAIT cells restored meningeal barrier integrity and suppressed microglial inflammation in the *Mr1*^{-/-} P301S mice.

Conclusions Our data indicate an important role for MAIT cells in regulating tau-pathology-related neuroinflammation and neurodegeneration.

[†]Yuanyue Zhang, Zhi Yang, Na Jiang have contributed equally to this work.

*Correspondence:

Qi Yang

qy117@rwjms.rutgers.edu

¹ Child Health Institute of New Jersey, Rutgers Robert Wood Johnson Medical School, 89 French St, New Brunswick, NJ 08901, USA

² Rutgers Institute for Translational Medicine and Science, Rutgers Robert Wood Johnson Medical School, New Brunswick, NJ 08901, USA

³ Department of Cell Biology and Neuroscience, Rutgers University, Piscataway, NJ 08854, USA

⁴ Department of Pediatrics, Johnson Medical School, Rutgers Robert Wood, New Brunswick, NJ 08901, USA



Background

Aberrant aggregation of misfolded microtubule-associated protein tau is a prominent feature of neurodegenerative disorders [1]. Previous studies have shown that the density of neurofibrillary tangles, which are intracellular aggregates of hyperphosphorylated tau, correlates with the severity of cognitive decline in Alzheimer's disease patients [2, 3]. Recent research suggested a complex interplay between tau pathology and neuroinflammation. Notably, microglial inflammation has been observed in mice carrying human tau mutants associated with degenerative tau pathologies, suggesting that tau-induced pathologies can trigger neuroinflammation [4]. Conversely, reactive microglia and its products may also exacerbate tau pathology and associated neurodegeneration [5–8].

Moreover, recent studies suggest that non-microglial immune cells, such as lymphocytes, may play a role in modulating tau pathology-related neuroinflammation and neurodegeneration [5]. CD8⁺ T cells infiltrate the brain parenchyma in Alzheimer's disease patients, as well as in 3D human neuroimmune culture derived from stem cells from AD patients and in mouse models with tauopathy [5, 9–12]. Increased infiltration of CD8⁺ T cells into 3-D human neuroimmune culture led to increased microglial activation, neuroinflammation and neurodegeneration [9]. Depletion of CD8⁺ T cells has also been shown to reduce tau pathology and prevent tau-mediated neurodegeneration in mouse models [5]. However, the roles of other lymphocyte subsets in regulating tau pathology and neurodegeneration remain largely unexplored.

The brain parenchyma is protected by complicated barrier structures, including blood brain barriers (BBB), choroid plexus, and meninges [13, 14]. Various immune cells are enriched in these brain barrier regions. We recently found that MAIT cells, a subset of microbiota-responsive innate-like T cells, were present in the leptomeninges and secreted many antioxidant proteins to protect meningeal barrier integrity [15]. MAIT cell-deficient mice exhibited notable meningeal barrier leakage, which inflamed the brain and disrupted cognitive function [15]. These data together demonstrate an important role for MAIT cells in protecting meningeal barrier integrity, and suggest that active maintenance of the meningeal barrier integrity by tissue-resident immune cells is essential for restricting neuroinflammation and for protecting cognitive function. However, whether this barrier-protective function influences tau-mediated neuroinflammation and neurodegeneration remains unknown.

In this study, we crossed MAIT cell-deficient mice (*Mr1*^{-/-}) with P301S mutant human tau transgenic mice to investigate the potential roles of MAIT cells in

regulating tau pathology, neuroinflammation, and neurodegeneration. We found that MAIT cells are present in the meninges of P301S mice and maintain high expression of antioxidant molecules. Our results indicate that the absence of MAIT cells leads to meningeal leakage, increased neuroinflammation, and exacerbated tau pathology and hippocampal atrophy in P301S transgenic mice. These findings suggest that MAIT cells play a role in modulating tau pathology and associated neuroinflammation and neurodegeneration.

Methods

Animals

P301S mice [4] and control mice on mixed C57BL/6 and C3H background were obtained from JAX laboratory. *Mr1*^{-/-} mice on C57BL/6N background were described previously [15, 16]. *Mr1*^{-/-} mice were generated by Taconic, and the validation and characterization of these mice were in the supplementary files of our previous publication [16]. P301S mice were bred with *Mr1*^{-/-} mice at the animal facility of Rutgers University. The offsprings were bred with each other and used in this study. Age and sex-matched female and male mice of 7 to 8-month-old were used. All animal experiments were performed according to protocols approved by the Institutional Animal Care and Use Committee at Rutgers University.

Age and sex-matched mice were randomly assigned to experimental and treatment groups. Experimenters were not blinded to the experimental groups. Mice with signs of major stress or sickness such as paralysis or notable reduction in food uptake were euthanized and excluded from the study. However, such incidents were rare in mice bred in our animal facility at the ages of this study. Except for snRNA-seq, at least two independent experiments were performed for each experiment. For immunofluorescence staining, imaging, and weight measurements, mice of the desired ages were euthanized on different dates, with staining or other measurements performed at the same time for each experiment. For flow cytometry analysis, mice with a birthdate difference of less than 7 days were euthanized at the same time for each independent experiment. For snRNA-seq, mice with a birthdate difference of less than 3 days were euthanized at the same time.

Flow cytometric analysis and fluorescence activated cell sorting (FACS)

Flow cytometric analysis and FACS sorting of MAIT cells were carried out as previously described [15]. Briefly, the meninges were carefully isolated from the outer dorsal cerebrum and inner calvaria surface. Hippocampus and cortex tissue were dissected on ice. The tissue was incubated for 20 min at 37 °C in HBSS containing 0.2 mg/

mL Liberase TM and 0.1 mg/mL DNase I to facilitate digestion. For analysis of meningeal cells, the digested tissue was passed through a 70 μ m cell strainer to generate a single-cell suspension. For analysis of hippocampus and cortex immune cells, Percoll centrifugation was performed to remove the debris, following enzymatic digestion. For flow cytometry, the cells were stained with MR1 tetramers along with antibodies targeting surface antigens for 30 min at 22 °C. The mouse MR1 5-OP-RU tetramers were obtained from the NIH Tetramer Core Facility. The MR1 tetramers were produced by the NIH Tetramer Core, as authorized for distribution by the University of Melbourne [17]. To define and characterize MAIT cells, surface markers used in the analysis included anti-TCR β (H57-597), anti-CD3 ϵ (145-2C11), anti-B220 (RA3-6B2), anti-NK1.1 (PK136), anti-CD11b (M1/70), anti-CD45 (104), anti-IL18R (A17071D), anti-Thy1.2 (53–2.1), and anti-IL7R (A7R34). Anti-B220, anti-NK1.1, and anti-CD11b antibodies were used to exclude B cells, NK cells, and myeloid cells to enhance MAIT cell identification. These antibodies were obtained from Biolegend, Thermo, or BD Biosciences. In flow cytometry and FACS sorting for QPCR analysis, meningeal MAIT cells were identified as CD45⁺ CD11b⁻ B220⁻ NK1.1⁻Thy1⁺ MR1tetramer⁺ CD3/TCR β ⁺, as we previously described [15, 16]. In some experiments, anti-IL18R and anti-IL7R antibodies were used for further characterize MAIT cells. Dead cells were excluded using DAPI (Thermo). For adoptive transfer experiments, no anti-CD3 or anti-TCR β antibodies were included to prevent cell activation, and donor MAIT cells were identified as CD45⁺ Thy1⁺ IL-18R⁺ MR1tetramer⁺.

For analysis and sorting of hippocampal microglia, hippocampal tissue was processed using the papain-based PierceTM Primary Neuron Isolation Kit (Thermo), according to the manufacturer's protocol. The cells were passed through a 70 μ m cell strainer and stained with surface markers, including anti-CD11b (M1/70) and anti-CD45 (104), before being sorted by FACS. Microglia was identified as CD11b^{med/low}CD45^{med/low} cells as we previously described [18–20]. In some experiments, anti-CD68 (FA-11), anti-CD86 (GL-1), anti-F4/80 (BM8), anti-MHCII (M5/114.15.2), and anti-CD11c (N418) were used to characterize microglia. Intracellular cytokine staining was performed as we previously described [16, 18–23]. Specifically, after digestion, cells were cultured with serum free RPMI medium for 4 h, and 1 μ M monensin was added for the last 2 h. The cells were then stained for surface markers to identify microglia, followed by intracellular staining with anti-TNF antibody (MP6-XT22). Intracellular cytokine staining was performed using the Cytofix/Cytoperm Kit (BD) as per the manufacturer's instructions.

Flow cytometry was performed using a 4-laser LSRII (BD Biosciences) or a 4-laser Cytex Aurora, and cell sorting was performed on a Cytex Aurora CS cell sorter.

Immunofluorescence staining

For immunofluorescence staining, mice were first perfused with 50 mL of PBS, followed by 50 mL of 4% paraformaldehyde. The brains were fixed overnight in 4% paraformaldehyde at 4 °C and then placed in 30% sucrose at 4 °C until the tissue sank. The brains were then embedded in OCT and stored at –80 °C. The brain sections were cut at 40 μ m using a CM1850 cryostat (Leica). The sections were stained with AT8 (Thermo) or anti-IBA1 (Fujifilm Wako) primary antibodies overnight at 4 °C, followed by labeling with AF594-conjugated donkey anti-mouse IgG (Thermo) or AF647-conjugated goat anti-rabbit IgG (Thermo) secondary antibodies. AT8 antibodies (Thermo Fisher) were used at a dilution of 1:100. Anti-IBA1 antibodies were used at a dilution of 1:1000. Images of the slides were captured using a BZ-X800 all-in-one fluorescence microscope (Keyence) with the BZ-X800 software. Images were analyzed by ImageJ.

Examination of hippocampus weight and volume

For measurement of the hippocampus weight, the hippocampal tissue was carefully isolated from each hemisphere and weighed in an EP tube. The weight was calculated by subtracting the weight of the tube before and after adding the hippocampal tissue. For hippocampus volume measurements, 40 μ m brain sections were cut sequentially and divided into four sets, with each set corresponding to one of the four consecutive cuts. One set of sections was used for hippocampus volume measurement. Sections were mounted with mounting medium containing DAPI and scanned by the Keyence microscope. Hippocampus volumes were calculated as total hippocampus areas of the sections \times 0.04 mm \times 4.

Adoptive transfer of MAIT cells

For adoptive transfer, meningeal MAIT cells (CD45⁺Thy1⁺IL18R^{hi}MR1-tetramer⁺) from 7-month-old P301S mice were sorted by FACS, and 1000 cells were transferred to 6 weeks old *Mr1*^{-/-} P301S mice intravenously. To minimize undesired cell activation, CD3 and TCR antibodies were not included for purification of donor cells for adoptive transfer. Centrifugation, FACS sorting and preparation for adoptive transfer, were carefully performed on ice or 4 °C. Meningeal leakage assays, immunofluorescence assays and hippocampus weight measurement were performed when recipient mice were around 7–8 months old.

Transcranial SR101 assay

Transcranial SR101 assays were performed as we previously described. For transcranial SR101 assay, mice were anesthetized with Ketamine and Xylazine. The skulls were exposed, and a light 4 mm diameter rubber ring was placed around the bregma. SR101 (2.5 mM in 15 μ l artificial CSF) was dropped into the rubber ring on top of the bregma, and was periodically replenished to prevent drying. At 20 min after SR101 administration, the skull was washed with artificial CSF. Mice were quickly euthanized and brain tissue was immediately obtained. 300 μ M coronal brain sections were quickly cut with a vibratome. Sections at 300 μ M–600 μ M away from the bregma were rapidly mounted on slides with a chamber filling with pre-chilled DAPI, and immediately imaged by Zeiss Axio Observer fluorescence. The Zeiss Zen 3.1 software (Zeiss) software was used to process the images. To quantify SR101 intensity, a 50 \times 100 μ M BOX was drawn at 50 μ M beneath the meninges, and the mean fluorescence intensity value was obtained.

Single nucleus RNA-seq

For single nucleus RNA-seq (snRNA-seq), the hippocampus was quickly isolated from fresh mouse brains on ice, and placed in Hibernate E medium (Gibco) supplemented with B27 (Gibco) and 1% GlutaMAX (Gibco). The tissue was homogenized using a Dounce grinder in pre-cooled RNase-free lysis buffer (10 mM Tris-HCl, 10 mM NaCl, 3 mM MgCl₂, 0.1% NonidetTM P40). The homogenization was performed with 15 strokes using a loose pestle, followed by 7 strokes using a tight pestle. The tissue was then lysed on ice for 15 min, and the solution was filtered through a 30 μ m cell strainer. The nuclei were washed, and myelin was removed using myelin removal kit (Miltenyi) according to the manufacturer's instructions. Libraries were prepared using 3' GEM gene expression kit (10xgenomics) following the manufacturer's instructions. Libraries were sequenced using a Novaseq. The scRNA-seq data were analyzed using the R package Seurat 4.3.0. Nuclei with fewer than 200 but more than 6500 genes, or more than 5% of mitochondrial genes, were filtered out. The R package DoubletFinder 2.0.3 was used to remove the doublets. Normalization of the data was achieved using the SCTransform function within Seurat. Cell clustering was performed using Uniform Manifold Approximation and Projection (UMAP). Microglia/macrophage population was sorted in silicon based on expression of positive markers of myeloid immune cells (e.g. *Itgam*, *Ptprc*) and the absence of markers associated with other immune cells (e.g. T/B/NK/ILC cells, monocytes, granulocytes). The microglia/macrophage population was then separated into distinct microglia subsets using UMAP. Gene markers for

each microglia subset and differentially expressed genes between microglia subsets of *Mr1*^{-/-} P301S and control *Mr1*^{+/+} P301S mice were identified using a threshold of false discovery rate of <0.05. The Gene Set Enrichment Analysis (GSEA) algorithm was utilized to access the enriched gene sets from differential genes. In brief, the differential gene expression of targeted groups was calculated with the R package limma 3.56.2. Then the differential genes were preranked by log₂FoldChange and subjected to the R package clusterProfiler 4.8.3. Results with p value <0.05, NES >1 and False discovery rate <0.25 were considered significant for GSEA analysis.

Multiplex cytokine assays and QPCR analysis

Multiplex cytokine assays were performed as we previously described [18, 20]. The brain was homogenized with 1 ml of PBS containing protease inhibitors using a tissue homogenizer. Concentrations of proinflammatory cytokines in brain homogenates were measured using LegendPlex kits, a kit for bead-based multiplex assays (Biolegend) [24], following the manufacturer's instructions.

For QPCR analysis, cells were sorted by FACS. cDNA was made by mRNA extraction and reverse transcription, or using a Cells-to-CT kit (Thermo). For mRNA extraction, mRNA was extracted using the RNeasy Plus Mini Kit (Qiagen), following the manufacturer's protocols. Complementary DNA (cDNA) was synthesized using SuperScript II Reverse Transcriptase (Thermo). For the Cells-to CT method, cDNA was generated using the Cells-to-CT kit (Thermo). qPCR was carried out using ABI pre-optimized TaqMan probes (Thermo).

Statistical analysis

For snRNA-seq data, Wilcoxon rank-sum test was used to determine significance of differentially expressed genes. False discovery rate less than 0.05 was considered significant. A Mann-Whitney U test was used to compare the differences in the percentages of subsets in each mouse for snRNA-seq data, and a p-value of less than 0.05 was considered significant. For GSEA analysis, results with p value <0.05, NES >1 and False discovery rate <0.25 were considered significant. For other experiments, student T test, or ANOVA test with Tukey's post-hoc test was used to determine the difference between two groups. A p-value of less than 0.05 was considered significant.

Results

MAIT cells are present in the meninges of P301S mutant human tau transgenic mice and retain expression of antioxidant molecules

Our recent work indicates that MAIT cells are present in adult mouse meninges where they secrete antioxidant

molecules to protect meningeal barrier integrity [15]. We performed flow cytometry analysis to examine MAIT cells in the meninges and brain parenchyma regions of P301S mutant human tau transgenic mice to determine whether tau pathology might affect MAIT cells abundance and distribution. MAIT cells were detected in the meninges of 7-month-old P301S mice, and their numbers were increased compared to age-matched control wildtype mice (Fig. 1A, B, Fig. S1). We did not observe significant infiltration of MAIT cells into the brain parenchymal regions such as hippocampus and cortex of P301S mice (Fig. 1B, C). Meningeal MAIT cells in 7-month-old wildtype mice expressed MAIT-characteristic markers such as IL7R, IL18R, and CD3e, verifying their identity (Fig. 1D). They expressed comparable mRNA levels of antioxidant molecules such as *Selenop*, *Selenof*, *Fth1*, *Tmsb4x*, and *Psap*, as MAIT cells in wildtype mice, indicating that MAIT cells in P301S mice might retain antioxidant activities (Fig. 1E). Thus, MAIT cells are increased in the meninges of P301S mice and retain expression of antioxidant molecules.

MAIT cell deficiency exacerbates tau pathology and hippocampus atrophy in P301S mice

Because MAIT cell development requires Mr1-expressing thymocytes for positive selection, *Mr1*^{-/-} mice lack MAIT cells due to failure in early development [25]. To examine the potential role of MAIT cells in regulating tau pathology, we crossed *Mr1*^{-/-} mice, which lacked MAIT cells, with P301S mice. As expected, MAIT cells were absent in the meninges of *Mr1*^{-/-} P301S mice (Fig. 2A, B). We examined tau pathology by immunofluorescence staining with AT8 antibody, which detects tau phosphorylation at the Ser202 and Thr205 positions [26, 27]. In mice bred in our animal facility, *Mr1*^{-/-} P301S mice exhibited significantly increased p-tau pathology compared to control *Mr1*^{+/+}P301S mice as early as 7 months old (Fig. 2C, D). At 8 months old, *Mr1*^{-/-} P301S mice showed a drastic increase in p-tau pathology compared with control *Mr1*^{+/+}P301S mice (Fig. 2E, F). These data suggest that MAIT cell deficiency might exacerbate tau pathology.

We noted that 7-month-old P301S mice directly purchased from JAX had higher levels of tau pathology compared to 7-month-old *Mr1*^{+/+}P301S mice bred in our institutional animal facility (Fig. S2). This might be due to genetic factors related to crossing, or environmental factors such as microbiota or nutrients or chronic exposure to environmental stimuli or stress. As expected, *Mr1*^{-/-} mice without human tau mutant transgenes did not exhibit significant AT8 staining in their hippocampus (Fig. S3A).

At 7.5 months of age, most control *Mr1*^{+/+}P301S mice did not yet exhibit notable hippocampus atrophy in mice bred in our animal facility (Fig. 2, G–I). In contrast, *Mr1*^{-/-} P301S mice displayed significant hippocampus atrophy at this age, indicating that the absence of MAIT cells may exacerbate tau-related neurodegeneration (Fig. 2, G–I). Of note, *Mr1*^{-/-} mice without human tau mutant transgene did not show hippocampus atrophy, suggesting that the increased neurodegeneration in *Mr1*^{-/-} P301S mice was associated with tau pathology (Fig. S3B, S3C). Together, these data indicate that MAIT cell deficiency may exacerbate neurodegeneration in P301S mice.

We next performed MAIT cell adoptive transfer experiments to verify the role of MAIT cells in regulating tau pathology and neurodegeneration (Fig. S4A). Adoptive transfer of MAIT cells partially restored MAIT cell numbers in the meninges (Fig. 2J, Fig. S4B). The adoptive transfer efficiency is around 30% to 50%. QPCR analyses revealed that the MAIT cells transferred into *Mr1*^{-/-} P301S mice expressed higher levels of the antioxidant molecule genes *Selenop* and *Fth1* compared to control MAIT cells from *Mr1*^{+/+}P301S mice (Fig. 2K, Fig. S4C). These data were consistent with our previous finding that reduced TCR exposure is associated with increased expression of antioxidant molecules in MAIT cells [15]. MAIT cell transfer significantly repressed p-tau pathology and hippocampus atrophy in *Mr1*^{-/-} P301S mice (Fig. 2, L–P). Together, these data indicate that MAIT cells repress tau pathology and neurodegeneration in adult P301S mice.

MAIT cell deficiency leads to meningeal leakage and increased microglial inflammation in P301S mice

We aim to understand the mechanisms by which MAIT cells suppress tau pathology and neurodegeneration in P301S mice. Previous studies indicate that increased microglial inflammation can exacerbate tau pathology and neurodegeneration in P301S mice [5, 28–30]. Our previous work suggests that MAIT cells protect meningeal barrier integrity via secretion of antioxidant molecules [15], which could help prevent noxious substances from entering the brain parenchyma and triggering enhanced microglial inflammation. We thus examined meningeal barrier integrity and microglial activities in *Mr1*^{-/-} P301S mice. At 7-months of age, a remarkable leakage in the meningeal barrier was observed in 7-month-old *Mr1*^{-/-} P301S mice, but not in control *Mr1*^{+/+} P301S mice (Fig. 3A, B). Immunofluorescence staining assays revealed markedly increased Iba1 reactivity in the hippocampus of *Mr1*^{-/-} P301S mice compared to *Mr1*^{+/+} P301S mice, indicating microglial/macrophage dysfunction (Fig. 3C, D). Flow cytometry analysis showed

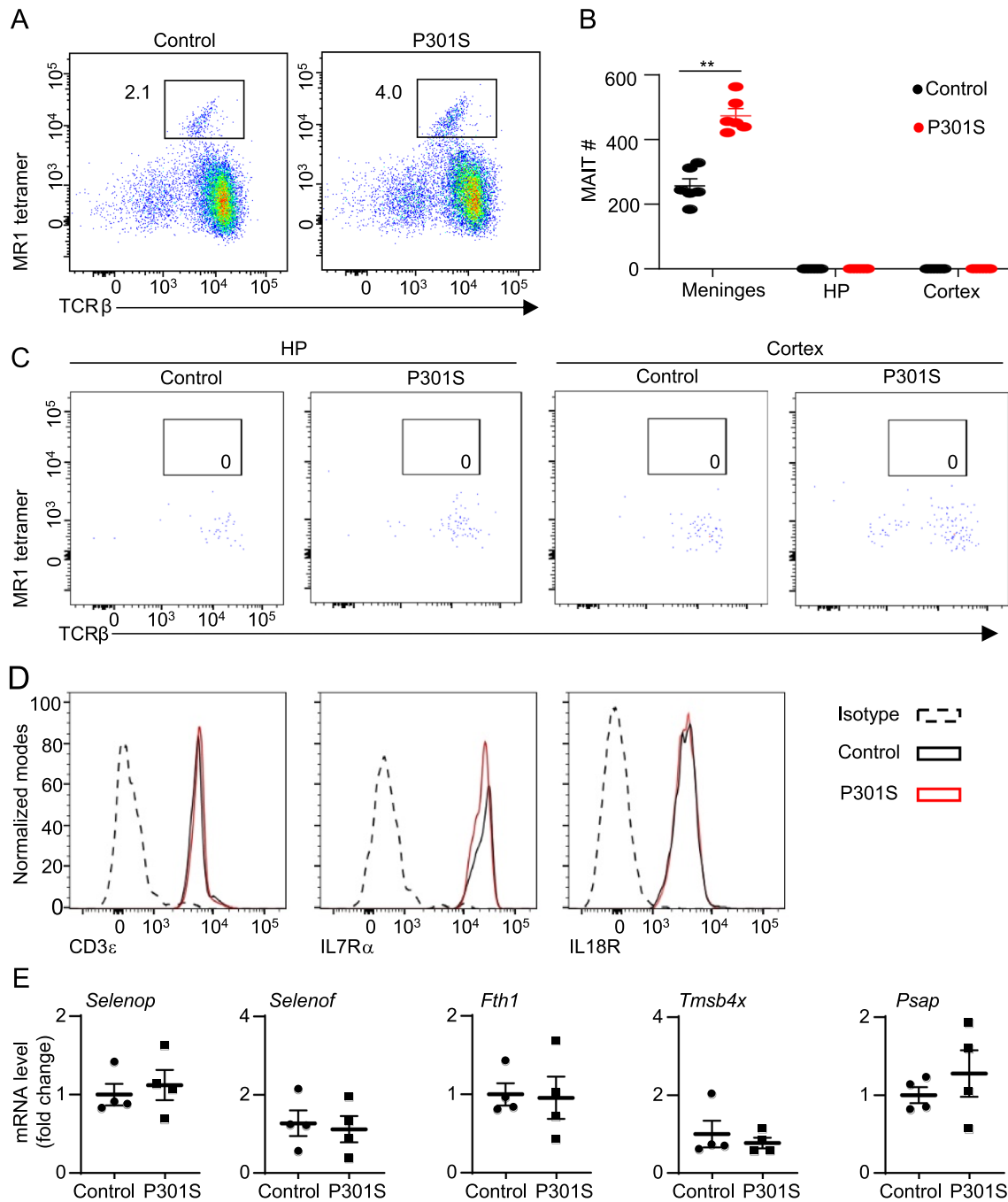


Fig. 1 MAIT cells are present in meninges of P301S mice and retain expression of antioxidant molecules. **A** Representative flow cytometry profiles of MAIT cells in the meninges of 7-month-old P301S mice and control wildtype mice. Plots were pre-gated on CD45⁺CD11b⁻B220⁻Thy1⁺ cells. **B** Numbers of MAIT cells in the meninges, hippocampus (HP), and cortex of 7-month-old P301S mice and wildtype mice. **C** Representative flow cytometry profiles of MAIT cells in the hippocampus and cortex. **D** Representative flow cytometry profiles showing expression of the indicated proteins by meningeal MAIT cells in P301S mice. Plots were pre-gated on meningeal MAIT cells in P301S mice. **E** mRNA levels of the indicated genes in meningeal MAIT cells of 7-month-old P301S mice and control wildtype mice. Data are from 6 mice per group pooled from 2 independent experiments **B**, or 4 independent experiments with 5 mice per group pooled per experiment **E**. Data were normalized to *Gapdh*. Error bars = mean \pm SEM. ****** $p < 0.01$. Sex information in Additional file 1

that microglia from the hippocampus *Mr1*^{-/-} P301S mice exhibited elevated expression of the proinflammatory cytokine TNF (Fig. 3E–G). Hippocampal microglia in *Mr1*^{-/-} P301S mice had increased expression of CD68 and F4/80, while expression of CD86, CD11b, MHCII, and CD11c remained unchanged (Fig. 3H, 3I, Supplementary S5). These data suggest that MAIT cell deficiency may increase microglia/macrophage inflammation in P301S mice.

Transfer of MAIT cells restored meningeal integrity in *Mr1*^{-/-} P301S mice, indicating that MAIT cells help prevent meningeal leakage in P301S mice (Fig. 3J, K). MAIT cell transfer reduced IBA1 reactivity in the hippocampus of *Mr1*^{-/-} P301S mice (Fig. 3L, M) and decreased the expression of TNF (Fig. 3N, O). These results indicate that the absence of MAIT cells leads to meningeal leakage and increased microglia inflammation in *Mr1*^{-/-} P301S mice.

Characterization of the transcriptomes of microglia in *Mr1*^{-/-} P301S mice

We next performed single-nucleus RNA-seq to examine the transcriptomes of microglia in the hippocampus of *Mr1*^{-/-} P301S mice and control *Mr1*^{+/+} P301S mice. Unsupervised UMAP divided hippocampal microglia/macrophage cells into several subsets (Fig. 4A, Additional File 2). All subsets expressed high levels of the immune-cell specific gene *Ptprc* (encoding CD45) and microglia/macrophage gene markers *Itgam* (encoding CD11b), *Adgre1* (encoding F4/80), and *Trem2* (Fig. S6). A subset expressed both microglia/macrophage and also neuron genes such as *Nrg3*, *Dlg2*, *Drxn3* (Fig. S6). These transcriptomes are possibly doublets, and are therefore

not included in further analysis (Fig. S6). The three most abundant microglia subsets differed in their expression of ribosome biogenesis genes encoding ribosome proteins, and were thus termed “M_ribo_hi”, “M_ribo_med”, and “M_ribo_lo” (Fig. 4A, B). In addition, a few minor subsets were detected (Fig. 4A). M_proliferating expressed high levels of proliferation markers such as *Ki67* (Fig. 4B). M_ISG expressed high levels of interferon stimulated genes (ISG) such as *Ifi44*, *Oasl2*, *Ifit2*, *Ifi204*, and *Ifit3*. M_magi2 was named by their expression of characteristic genes *Magi2*, but lacked significant expression of other non-microglia genes (Fig. 4B, Fig. S6, Additional file 2). Notably, a distinct subset of microglia appeared, expressing a high level of proinflammatory cytokines such as *Tnf*, *Il1a*, and *Il1b*, as well as proinflammatory chemokines such as *Ccl3* and *Ccl4* (Fig. 4A, B). We named this subset Inflammatory Microglia (M_inflammatory) (Fig. 4A, B). *Mr1*^{-/-} P301S mice had significantly higher percentages of M_inflammatory subset, compared to control *Mr1*^{+/+} P301S mice (Fig. 4C, D). The other microglia/macrophage subsets did not show significant difference in percentages between *Mr1*^{-/-} P301S mice and control *Mr1*^{+/+} P301S mice (Fig. 4C, D). Thus, *Mr1*^{-/-} P301S mice had accumulation of a distinctive subset of microglia expressing high levels of proinflammatory genes.

We performed a more thorough analysis of M_inflammatory cells. GSEA analysis revealed that these cells exhibit higher expression of genes associated with proinflammatory cytokine and chemokine pathways, as well as immune and inflammatory responses to toxic substances (Fig. 4E). Notably, the proinflammatory cytokine and chemokine genes *Tnf*, *Il1b*, *Ccl3*, and *Ccl4* were among the most significantly upregulated in M_inflammatory

(See figure on next page.)

Fig. 2 MAIT cells repress tau pathology and neurodegeneration in P301S mice. **A** Representative flow cytometry profiles of MAIT cells in the meninges of 7-month-old *Mr1*^{-/-} P301S mice and control *Mr1*^{+/+} P301S mice. Plots were pre-gated on CD45⁺CD11b⁻B220⁻Thy1⁺ cells. **B** Numbers of MAIT cells in the meninges of 7-month-old *Mr1*^{-/-} P301S mice and control *Mr1*^{+/+} P301S mice. **C** Immunofluorescence staining of p-Tau (antibody clone AT8) in the hippocampus DG of 7-month *Mr1*^{-/-} P301S mice and control *Mr1*^{+/+} P301S mice. **D** Percentages of AT8+ areas in the hippocampus DG of 7-month *Mr1*^{-/-} P301S mice and control *Mr1*^{+/+} P301S mice. **E** Immunofluorescence staining of p-Tau (antibody clone AT8) in the hippocampus DG of 8-month-old *Mr1*^{-/-} P301S mice and control *Mr1*^{+/+} P301S mice. **F** Percentages of AT8+ areas in the hippocampus of 8-month-old *Mr1*^{-/-} P301S mice and control *Mr1*^{+/+} P301S mice. **G** Representative images of hippocampus of 7.5-month *Mr1*^{-/-} P301S mice and control *Mr1*^{+/+} P301S mice. **H** Weight of the hippocampus in 7.5-month *Mr1*^{-/-} P301S mice and control *Mr1*^{+/+} P301S mice. **I** Volumes of the hippocampus in 7.5-month *Mr1*^{-/-} P301S mice and control *Mr1*^{+/+} P301S mice. **J** MAIT cells were transferred to 6-week-old *Mr1*^{-/-} P301S mice. Number of MAIT cells in meninges of recipient mice was measured by flow cytometry analysis, when the mice were 8-months old. **K** mRNA levels of *Selenop* in MAIT cells purified from 8-month-old *Mr1*^{-/-} P301S mice with adoptive transfer of MAIT cells, and control MAIT cells purified from 8-month-old *Mr1*^{+/+} P301S mice without adoptive transfer. **L** Immunofluorescence staining of p-Tau (antibody clone AT8) in the hippocampus DG of 8-month *Mr1*^{-/-} P301S mice with adoptive transfer of MAIT cells or PBS. **M** Percentages of AT8+ areas in the hippocampus DG of 8-month *Mr1*^{-/-} P301S mice with adoptive transfer of MAIT cells or PBS. **N** Representative images of hippocampus of 7.5-month *Mr1*^{-/-} P301S mice with adoptive transfer of MAIT cells or PBS. **O** Weight of the hippocampus in 7.5-month-old *Mr1*^{-/-} P301S mice with adoptive transfer of MAIT cells or PBS. **P** The volumes of hippocampus in 7.5-month-old *Mr1*^{-/-} P301S mice with adoptive transfer of MAIT cells or PBS. Data are from 6 mice per group pooled from 2 independent experiments (**B, J, K**), or are from 8 mice per group representative of two independent experiments (**D, F, M**), or are from 10 mice per group pooled from more than two independent experiments (**H, I, O, P**). Error bars = mean ± SEM. ***p* < 0.01; **p* < 0.05. Sex information in Additional file 1

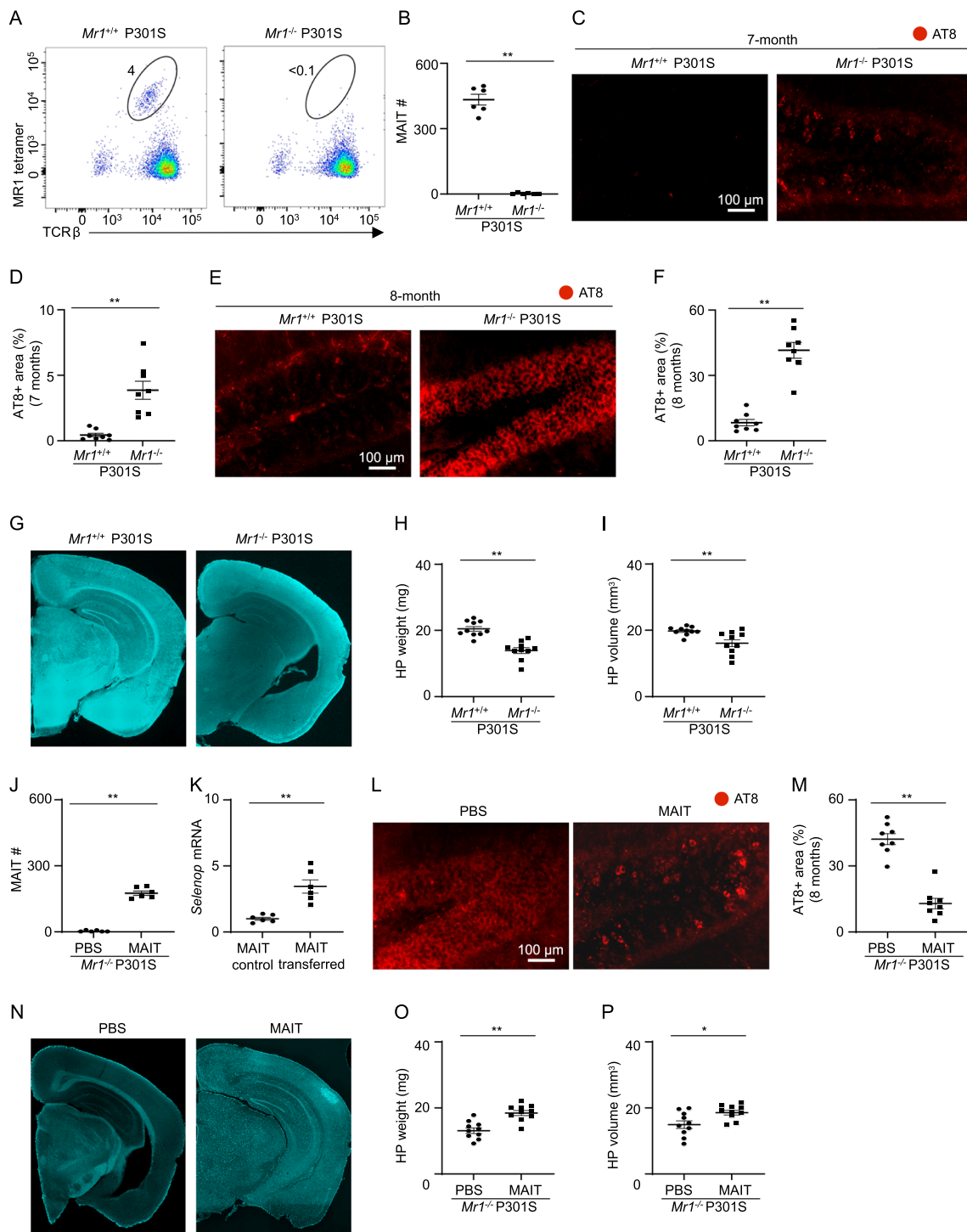


Fig. 2 (See legend on previous page.)

cells (Fig. 4F). In addition to these proinflammatory mediators, these cells showed elevated expression of other genes related to responses to toxic substances (e.g. *Slc2a1*, *Mapkapk2*, *Etf1*, *Srgn*, *Txnrd1*, *Sqstm1*, *Nfkb-ia*), suggesting they may be exposed to higher levels of

noxious substances (Fig. 4G). Together, M_inflammatory cells display a pro-inflammatory profile characterized by a distinct transcriptomic signature.

We also examined the transcriptomal changes of other microglia subsets in *Mr1*^{-/-} P301S mice. We

focused on the three major microglia subsets (M_ribo_hi, M_ribo_Med, M_ribo_low). Notable similarity was observed in the transcriptomal changes in all these three subsets between *Mr1*^{-/-} P301S and control *Mr1*^{+/+} P301S mice (Fig. 5, A-F). Specifically, the genes upregulated in each microglia subset in *Mr1*^{-/-} P301S mice were found to be enriched in genes related with lipoprotein assembly and clearance, ribosomal proteins, and inflammatory responses to toxic substances (Fig. 5, A-F). *ApoE*, a lipoprotein gene highly expressed in human microglia of Alzheimer's disease patients [31], was expressed much higher in all the three main microglia subsets in *Mr1*^{-/-} P301S mice compared to those in *Mr1*^{+/+} P301S mice (Fig. 5B, D, F). A few other lipoprotein assembly and clearance related genes, such as *Lpl*, *Apoc1*, *Abcg1*, *Nceh1*, *Npc2*, were also significantly upregulated in all three main microglia subsets in *Mr1*^{-/-} P301S mice compared to *Mr1*^{+/+} P301S mice. A variety of ribosome biogenesis genes (e.g. *Rps18*, *Rpl10a*, *Rps28*, *Rpl41*, *Rpl36a*, *Rpl39*) were also expressed higher in all the three main microglia subsets in *Mr1*^{-/-} P301S mice (Fig. 5, A-F). These genes encode ribosomal proteins, and their increased expression suggests enhanced ribosome biogenesis and gene translation. In addition, microglia in *Mr1*^{-/-} P301S mice expressed higher levels of genes related to immune and inflammatory responses to toxic substances indicating that they might be exposed to higher levels of noxious substances (Fig. 5, A-F). Proinflammatory chemokines and cytokines, such as *Ccl3*, *Ccl4*, *Il1b*, and *Tnf*, were among the gene sets associated with responses to toxic substances. These proinflammatory chemokine and cytokine genes were upregulated in microglia of

Mr1^{-/-} P301S mice (Fig. 5B, D, F). Together, microglia in *Mr1*^{-/-} P301S mice exhibit a proinflammatory profile.

Our *Mr1*^{-/-} mice were characterized and validated in previous studies. Of note, our snRNA-seq data detected *Mr1* expression in cells from *Mr1*^{-/-} P301S mice, but not in cells from *Mr1*^{+/+} mice (Fig. S7). These data verify the absence of MR1 expression in *Mr1*^{-/-} mice.

We next performed QPCR to verify the gene expression in microglia that were FACS-sorted from the hippocampus of *Mr1*^{-/-} P301S mice and control *Mr1*^{+/+} P301S mice. Of note, *ApoE* was greatly upregulated in the hippocampal microglia of *Mr1*^{-/-} P301S mice, compared to those in control *Mr1*^{+/+} P301S mice (Fig. 6A). Expression of another lipoprotein *Apoc1* was also increased in microglia from the hippocampus of *Mr1*^{-/-} P301S mice. Microglia from *Mr1*^{-/-} P301S mice also exhibited increased expression of the representative ribosome biogenesis gene *Rps18*, as well as genes that were upregulated in responses to toxic substances such as *Spp1* and *Rsad2*. Transfer of MAIT cells reduced the expression of these genes in microglia from *Mr1*^{-/-} P301S mice (Fig. 6B), verifying that the presence of MAIT cells repress the expression of these genes in hippocampus microglia of P301S mice. We then performed multiplex cytokine assays to verify whether the protein concentrations of proinflammatory cytokines in the brain homogenates of *Mr1*^{-/-} P301S mice and control *Mr1*^{+/+} P301S mice. The concentrations of proinflammatory cytokines including IL1b, IL1a, and TNE, were significantly increased in the brain homogenates of *Mr1*^{-/-} P301S mice (Fig. 6C). Adoptive transfer of MAIT cells reduced the concentrations of these proinflammatory cytokines, indicating that

(See figure on next page.)

Fig. 3 MAIT cells protect meningeal barrier integrity and repress proinflammatory cytokine expression from microglia. **A** Brain vibratome sections were obtained from 7-month-old *Mr1*^{-/-} P301S mice and control *Mr1*^{+/+} P301S mice with transcranial administration of SR101. Representative imaging of sections at 300 μ M to 600 μ M lateral to bregma. **B** Quantification of fluorescence intensity of SR101 at 50 μ M below the leptomenigeal cells in the brain vibratome sections of 7-month-old *Mr1*^{-/-} P301S mice and control *Mr1*^{+/+} P301S mice. **C** Immunofluorescence staining of IBA1 in hippocampus DG of 7-month *Mr1*^{-/-} P301S mice and control *Mr1*^{+/+} P301S mice. **D** Percentages of IBA1 + areas in the hippocampus DG of 7-month *Mr1*^{-/-} P301S mice and control *Mr1*^{+/+} P301S mice. **E** Representative flow cytometry profile showing gating strategy of microglia in the hippocampus. **F** Representative flow cytometry profiles showing expression of TNF in microglia in the hippocampus of 7-month-old *Mr1*^{-/-} P301S mice and control *Mr1*^{+/+} P301S mice. **G** Mean fluorescence intensity of TNF in microglia in the hippocampus of 7-month-old *Mr1*^{-/-} P301S mice and control *Mr1*^{+/+} P301S mice. **H** Representative flow cytometry profiles showing expression of the indicated molecules by hippocampus microglia in 7-month-old *Mr1*^{-/-} P301S mice and control *Mr1*^{+/+} P301S mice. **I** Mean fluorescence intensity of the indicated molecules in microglia in the hippocampus of 7-month-old *Mr1*^{-/-} P301S mice and control *Mr1*^{+/+} P301S mice. **J** MAIT cells were transferred to 6-week-old *Mr1*^{-/-} P301S mice. Brain vibratome sections were obtained in mice with transcranial administration of SR101, when mice were 7-month-old. Representative images for mice with adoptive transfer of MAIT cells or PBS control. **K** Quantification of fluorescence intensity of SR101 at 50 μ M below the leptomenigeal cells in mice with adoptive transfer of MAIT cells or PBS control. **L** Immunofluorescence staining of IBA1 in the hippocampus DG of 7-month-old *Mr1*^{-/-} P301S mice with adoptive transfer of MAIT cells or PBS. **M** Percentages of IBA1 + areas in the hippocampus of 7-month-old *Mr1*^{-/-} P301S mice with adoptive transfer of MAIT cells or PBS. **N** Representative flow cytometry profiles showing expression of TNF in microglia in the hippocampus of 7-month-old *Mr1*^{-/-} P301S mice with adoptive transfer of MAIT cells or PBS. **O** Mean fluorescence intensity of TNF in the hippocampus of 7-month *Mr1*^{-/-} P301S mice with adoptive transfer of MAIT cells or PBS. Data are from 4–6 mice per group, representative of 2 independent experiments. Error bars = mean \pm SEM. ***p* < 0.01, **p* < 0.05. Sex information in Additional file 1

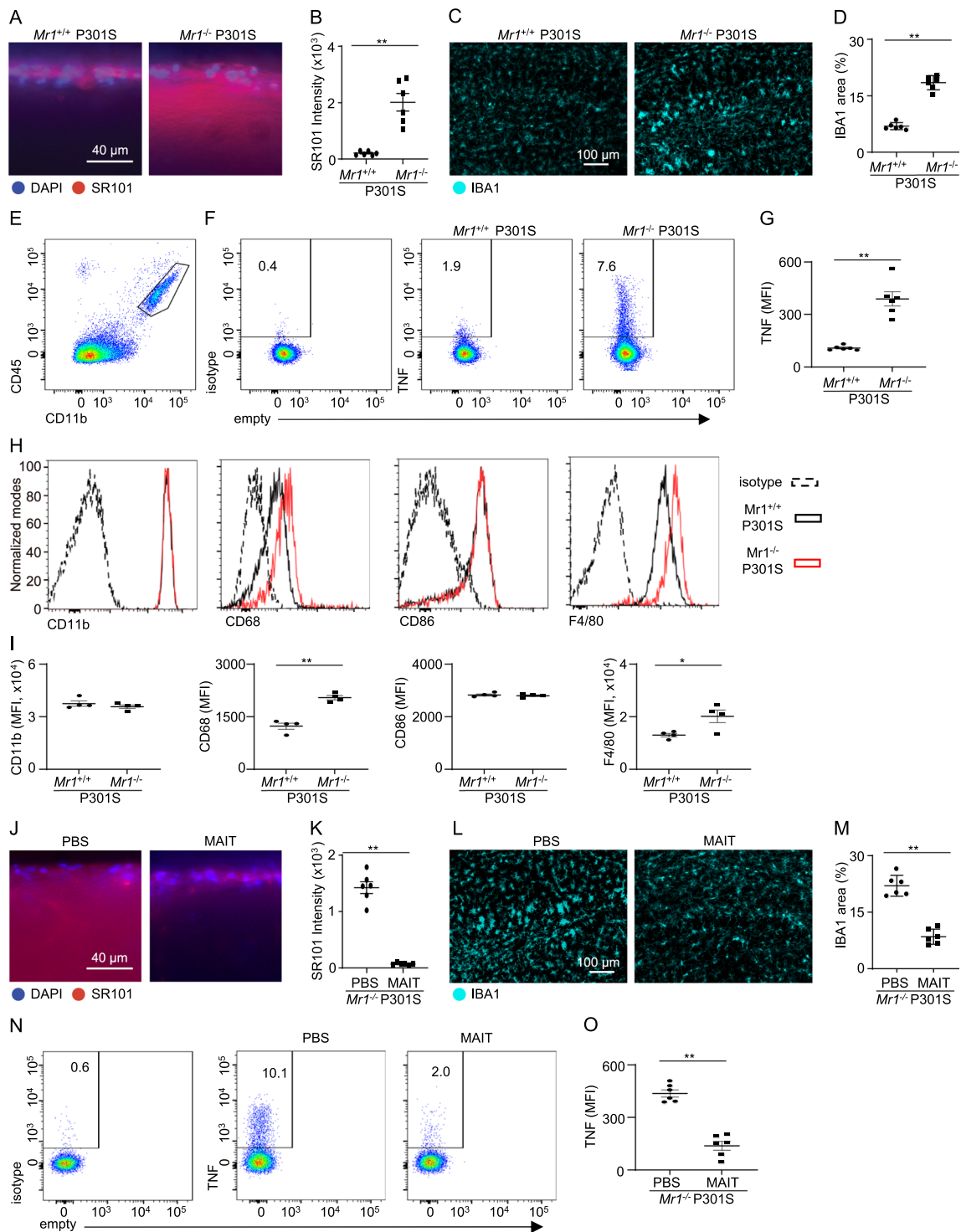


Fig. 3 (See legend on previous page.)

the presence of MAIT cells repressed neuroinflammation in *Mr1^{-/-}* P301S mice (Fig. 6D). Together, these data verify that MAIT cells repress microglial inflammation in P301S mice.

Discussion

In this study, we revealed an important role of MAIT cells in regulating tau pathology and neurodegeneration in P301S transgenic mice and investigated the underlying

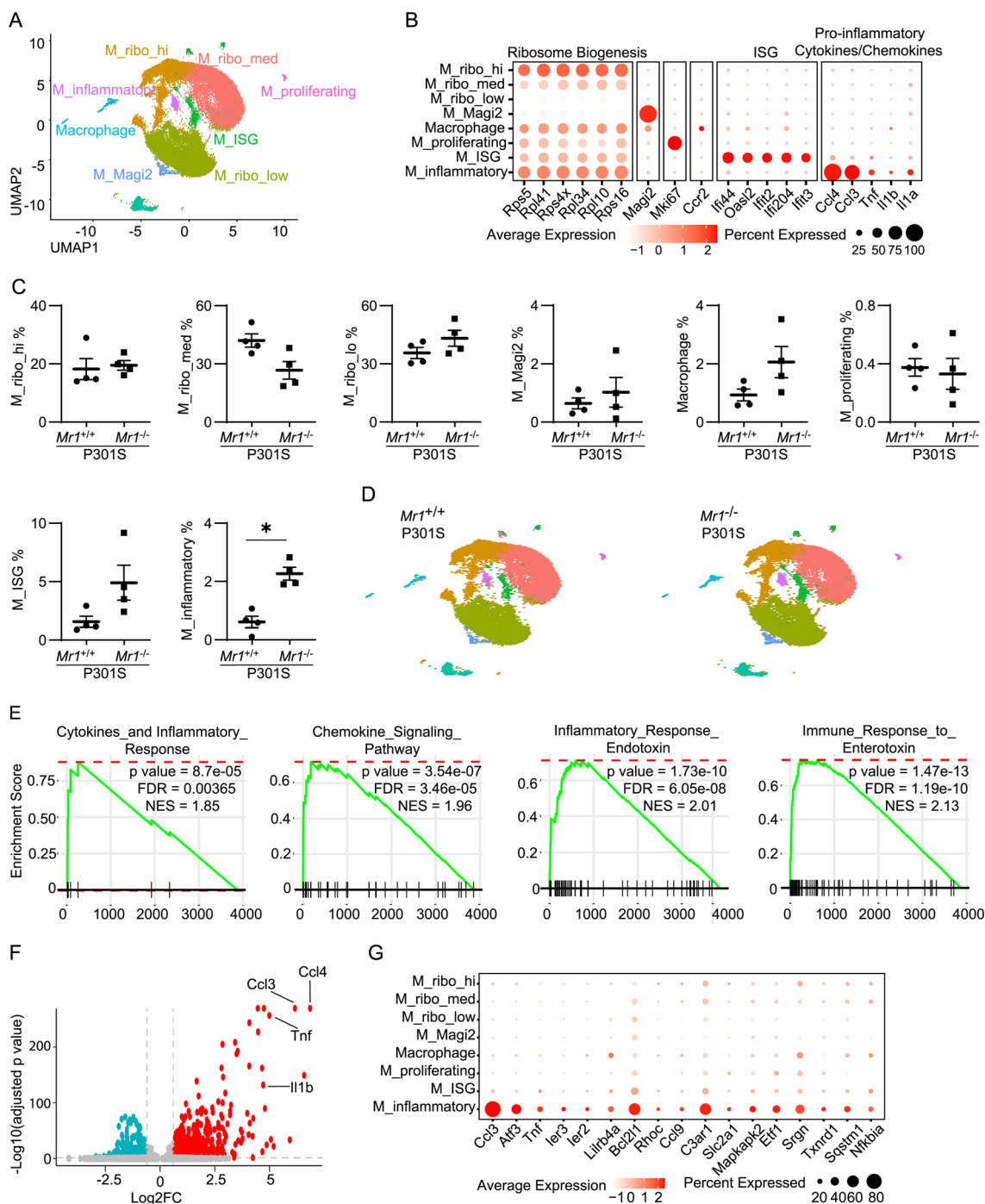


Fig. 4 Transcriptome profiles of hippocampus microglia in 7-month-old *Mr1*^{-/-} P301S mice and control *Mr1*^{+/+} P301S mice **A** UMAP plot showing different clusters of microglia/macrophage in the hippocampus of 7-month-old mice by single-nucleus RNA-seq analysis. Shown are all microglia/macrophage pooled from four 7-month-old *Mr1*^{-/-} P301S mice and four control *Mr1*^{+/+} P301S mice. **B** Dot plots showing expression levels of the indicated genes of each subset. **C** Percentages of each microglia and macrophage subset. **D** UMAP plots showing different clusters of microglia/macrophage in the hippocampus of 7-month-old *Mr1*^{-/-} P301S mice and control *Mr1*^{+/+} P301S mice separately. **E** Enrichment of the indicated gene sets in *M_inflammatory* cells versus the other microglia/macrophage subsets. **F** Volcano plots depict genes that are significantly upregulated or downregulated in *M_inflammatory* cells compared to other microglia/macrophage cells. **G** Dot plots showing expression levels of the indicated genes of each subset. Data are from 4 mice per group. Sex information in Additional file 1. Error bars = mean ± SEM. **p* < 0.05. Sex information in Additional file 1

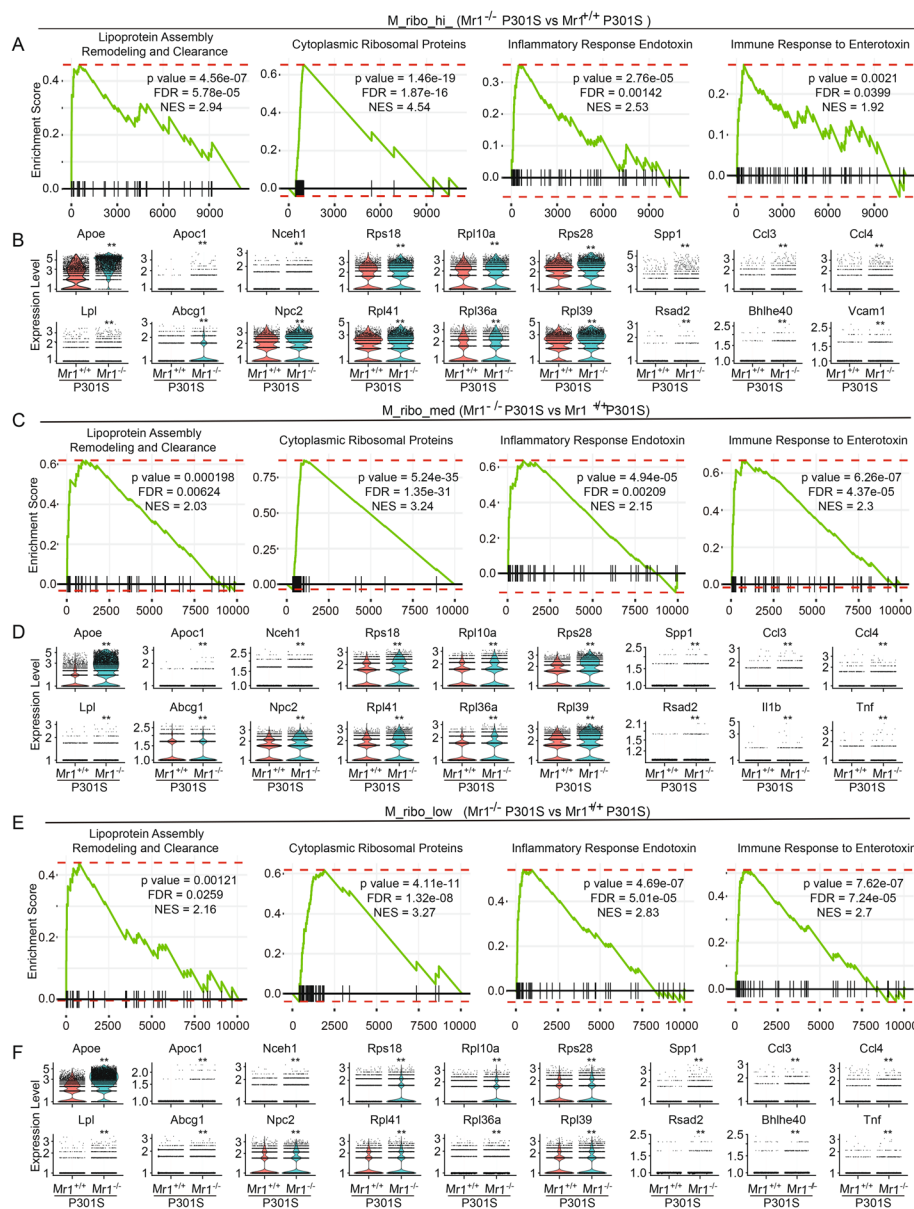


Fig. 5 Comparison of gene expression of the main microglia subset of hippocampus microglia between 7-month-old *Mr1*^{-/-} P301S mice and control *Mr1*^{+/+} P301S mice. **A** Enrichment of the indicated gene sets in *M_ribo_hi* cells from 7-month-old *Mr1*^{-/-} P301S mice and control *Mr1*^{+/+} P301S mice. **B** Violin plots show expression of representative genes that were differentially expressed in *M_ribo_hi* cells between 7-month-old *Mr1*^{-/-} P301S mice and control *Mr1*^{+/+} P301S mice. **C** Enrichment of the indicated gene sets in *M_ribo_med* cells from 7-month-old *Mr1*^{-/-} P301S mice and control *Mr1*^{+/+} P301S mice. **D** Violin plots show expression of representative genes that were differentially expressed in *M_ribo_med* cells between 7-month-old *Mr1*^{-/-} P301S mice and control *Mr1*^{+/+} P301S mice. **E** Enrichment of the indicated gene sets in *M_ribo_low* cells from 7-month-old *Mr1*^{-/-} P301S mice and control *Mr1*^{+/+} P301S mice. **F** Violin plots show expression of representative genes that were differentially expressed in *M_ribo_low* cells between 7-month-old *Mr1*^{-/-} P301S mice and control *Mr1*^{+/+} P301S mice. Data are from 4 mice per group

mechanisms. Our findings demonstrated that MAIT cells are present in the meninges and express antioxidant molecules. We showed that the deficiency of MAIT cells leads to meningeal barrier leakage and examined microglial dysfunction in P301S mice lacking MAIT cells. Our data together suggest an important role for MAIT

cells in repressing tau related neuroinflammation and neurodegeneration.

Increasing evidence indicates that lymphocytes particularly T cells may contribute to the regulation of brain homeostasis and neurodegeneration [5, 9–12]. MAIT cells are a unique type of innate-like T cells that

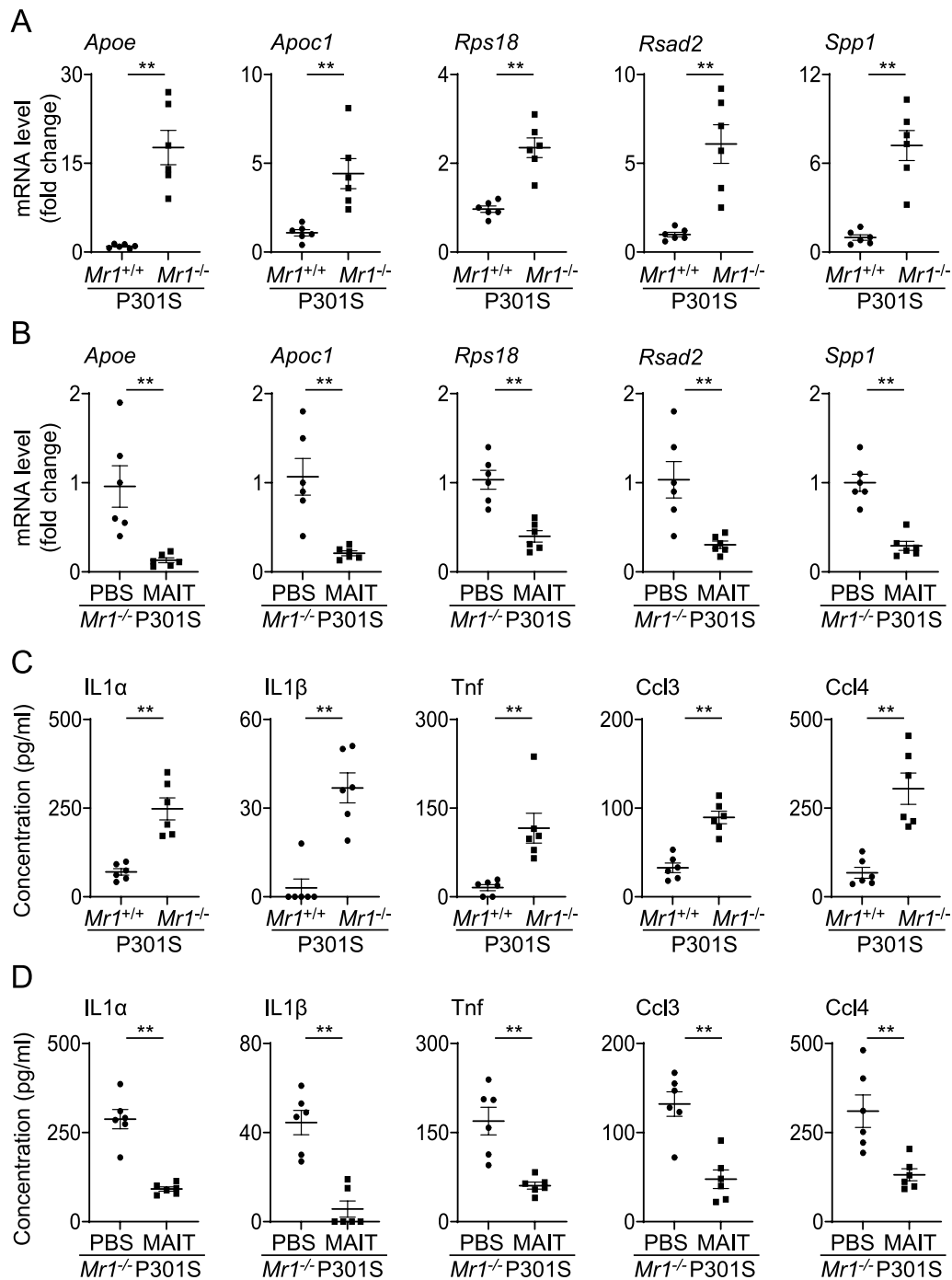


Fig. 6 The presence of MAIT cells alters gene expression in microglia and represses proinflammatory cytokine concentrations in P301S mice. **A** mRNA levels of the indicated genes in microglia sorted from the hippocampus of 7-month-old *Mr1*^{-/-} P301S mice and control *Mr1*^{+/+} P301S mice. **B** mRNA levels of the indicated genes in microglia sorted from the hippocampus of 7-month-old *Mr1*^{-/-} P301S mice with adoptive transfer of MAIT cells or PBS. **C** Concentrations of the indicated cytokines in the brain homogenate of 7-month-old *Mr1*^{-/-} P301S mice and control *Mr1*^{+/+} P301S mice. **D** Concentrations of the indicated cytokines in the brain homogenate of 7-month-old *Mr1*^{-/-} P301S mice with adoptive transfer of MAIT cells or PBS. Data are from 6 mice per group, representative of 2 independent experiments. Error bars = mean \pm SEM. ** $p < 0.01$. Sex information in Additional file 1

are abundant in humans [32, 33]. Our previous work suggested that MAIT cells are present in the meninges of adult wildtype mice, where they express antioxidant molecules that help maintain meningeal barrier integrity [15]. We hypothesized that this barrier protective function is important to regulate tau pathology and neurodegeneration. In this study, we found that *Mr1*^{-/-} P301S mice that lack MAIT cells exhibited meningeal leakage, microglial inflammation, and exacerbated tau pathology and neurodegeneration, compared to *Mr1*^{+/+} P301S mice. The MR1 molecule is a highly conserved molecule specialized in antigen presentation [17, 34–37]. Given its unique tertiary structure, we do not expect that the MR1 molecule has other significant functions not related to MAIT cells or other Mr1-restrictive T cells. In this study, we performed MAIT cell adoptive transfer experiments to verify the functional capability of MAIT cells in vivo. The transfer of MAIT cells restored meningeal barrier integrity and suppressed microglial inflammation and neurodegeneration in the *Mr1*^{-/-} P301S mice. While we cannot yet establish a causal relationship among the phenotypic changes in *Mr1*^{+/+} P301S mice, our data collectively provide insights into a role of MAIT cells in regulating neuroinflammation and neurodegeneration in the context of tau pathology. Of note, the abundance of MAIT cells is highly variable and influenced by the microenvironment, particularly the microbiota [38–40]. Future research exploring the relationship between gut microbiota, MAIT cell development, and neurodegeneration could provide further insights into the mechanisms underlying neurodegenerative diseases.

Previous work indicates reactive microglia may lead to neurodegeneration in in vitro 3D human neuroimmune culture and exacerbate tau pathology in transgenic mouse models [5–9]. Conversely, increased tau pathology also induces microglia inflammation [4]. In our study, we observed a remarkable increase in proinflammatory cytokines in the hippocampus of *Mr1*^{-/-} P301S mice, accompanied by a pronounced proinflammatory profile of microglia. Tau pathology is also notably increased in *Mr1*^{-/-} P301S mice. While our results do not establish a causal relationship between elevated tau pathology and increased neuroinflammation in *Mr1*^{-/-} P301S mice, we hypothesize that the elevated tau pathology and increased neuroinflammation might form a positive feedback loop, together exacerbating neurodegeneration. Future research to dissect the precise mechanistic pathways might be worthwhile.

Our scRNA_seq analysis identified a distinct microglia subset that accumulated in the hippocampus of *Mr1*^{-/-} P301S mice, which we termed M_inflammatory. These cells exhibited proinflammatory phenotype. They mostly closely resemble the Microglia_chemokine mentioned

in an earlier report [41]. However, because Microglia_chemokine cells were extremely rare in wildtype mice, detailed description of Microglia_chemokine was yet lacking in the earlier study, except that these cells express high levels of chemokines [41]. Here, we performed extensive transcriptomic analysis of M_inflammatory cells, and found that they express high levels of proinflammatory cytokines and genes related to immune and inflammatory responses to toxic substances. Our data indicate that M_inflammatory may represent a proinflammatory microglial subset that emerges in response to increased exposure to noxious substance. Further exploration of these cells in other pathological contexts and their specific roles in brain function and neurodegeneration might be an important avenue for future research.

Our study has several limitations. The microglia analyses in this study were performed at a relatively early age in which tau pathology was yet moderate. While our results focused on the early changes in microglia, future research exploring longer time points might provide insights into the role of MAIT cells in regulating neuroinflammation along the disease progression. Additionally, our flow cytometry analyses did not reveal significant infiltration of MAIT cells into the brain parenchyma of P301S mice. The experimental procedures involved in flow cytometry analyses, such as enzymatic digestion and Percoll centrifugation, may inevitably cause cell loss or damages to TCR structures. Therefore, we cannot exclude the possibility that a small number of MAIT cells might be present in the brain parenchyma of adult P301S or wildtype mice. Moreover, the abundance of MAIT cells is highly dependent on microbiota, and thus it is expected that MAIT cell abundance may vary across mice bred in different animal facilities at different institutions. Additionally, the abundance of MAIT cells may change in certain pathological conditions. Previous work indicates MAIT cell infiltration into the brain parenchyma of 5xFAD mice, where they interact with microglia to influence Amyloid b pathology [42]. Future studies to understand the ontogeny and functional similarities and divergence between meningeal MAIT cells and those infiltrating the brain parenchyma might be worthwhile.

Conclusion

In conclusion, we report that MAIT cells were present in the meninges of P301S mutant human tau transgenic mice and retain expression of antioxidant molecules. The absence of MAIT cells exacerbates tau pathology and neurodegeneration in P301S mice. MAIT cells protect meningeal integrity and repress neuroinflammation in P301S mice. Together, these results indicate that

a role of MAIT cells in regulating neurodegenerative tau pathology.

Abbreviations

MAIT	Mucosal-associated invariant T cells
MR1	MHCI-related
APC	Antigen presenting cells
FACS	Fluorescence activated cell sorting
snRNA-seq	Single nucleus RNA sequencing
UMAP	Uniform manifold approximation and projection
GSEA	Gene set enrichment analysis
cDNA	Complementary DNA (cDNA)
M_inflammatory	Inflammatory microglia
ISG	Interferon stimulated gene

Supplementary Information

The online version contains supplementary material available at <https://doi.org/10.1186/s12974-025-03413-7>.

Additional file 1.

Additional file 2.

Additional file 3.

Acknowledgements

We thank Drs. Zhiping Pang and Arnold Rabson for helpful discussion.

Author contributions

Y.Z., Z.Y., J.N., X.T., P.J., G.C., and Q.Y. performed the experiments and analyzed the data. Z.Y. performed bioinformatics analysis. Y.Z., Z.Y., J.N., and Q.Y. wrote the manuscript. All authors approved the manuscript.

Funding

This work was supported by the U.S. National Institutes of Health Grants R01HL155021 (QY), RF1AG078459 (QY), and support to the Child Health Institute of New Jersey from the Robert Wood Johnson Foundation (Grant #74260).

Availability of data and materials

snRNA-seq data were deposited at Gene Expression Omnibus (accession number GSE285822).

Declarations

Ethics approval and consent to participate

All animal experiments were approved by Rutgers Institutional Animal Care and Use Committee.

Consent for publication

Not applicable.

Competing interests

Q.Y. reports a patent WO2020197984A1. The authors declare no other conflicts of interest.

Received: 5 January 2025 Accepted: 8 March 2025

Published online: 20 March 2025

References

- Samudra N, Lane-Donovan C, VandeVrede L, Boxer AL. Tau pathology in neurodegenerative disease: disease mechanisms and therapeutic avenues. *J Clin Invest*. 2023. <https://doi.org/10.1172/JCI168553>.
- Gomez-Isla T, Hollister R, West H, Mui S, Growdon JH, Petersen RC, Parisi JE, Hyman BT. Neuronal loss correlates with but exceeds neurofibrillary tangles in Alzheimer's disease. *Ann Neurol*. 1997;41:17–24.
- Arriagada PV, Growdon JH, Hedley-Whyte ET, Hyman BT. Neurofibrillary tangles but not senile plaques parallel duration and severity of Alzheimer's disease. *Neurology*. 1992;42:631–9.
- Yoshiyama Y, Higuchi M, Zhang B, Huang SM, Iwata N, Saido TC, Maeda J, Suhara T, Trojanowski JQ, Lee VM. Synapse loss and microglial activation precede tangles in a P301S tauopathy mouse model. *Neuron*. 2007;53:337–51.
- Chen X, Firulyova M, Manis M, Herz J, Smirnov I, Aladyeva E, Wang C, Bao X, Finn MB, Hu H, et al. Microglia-mediated T cell infiltration drives neurodegeneration in tauopathy. *Nature*. 2023;615:668–77.
- Fan Q, He W, Gayen M, Benoit MR, Luo X, Hu X, Yan R. Activated CX3CL1/Smad2 signals prevent neuronal loss and Alzheimer's tau pathology-mediated cognitive dysfunction. *J Neurosci*. 2020;40:1133–44.
- Maphis N, Xu G, Kokiko-Cochran ON, Jiang S, Cardona A, Ransohoff RM, Lamb BT, Bhaskar K. Reactive microglia drive tau pathology and contribute to the spreading of pathological tau in the brain. *Brain*. 2015;138:1738–55.
- Ghosh S, Wu MD, Shaftel SS, Kyrkanides S, LaFerla FM, Olschowka JA, O'Banion MK. Sustained interleukin-1beta overexpression exacerbates tau pathology despite reduced amyloid burden in an Alzheimer's mouse model. *J Neurosci*. 2013;33:5053–64.
- Jorfi M, Park J, Hall CK, Lin CJ, Chen M, von Maydell D, Kruskop JM, Kang B, Choi Y, Prokopenko D, et al. Infiltrating CD8(+) T cells exacerbate Alzheimer's disease pathology in a 3D human neuroimmune axis model. *Nat Neurosci*. 2023;26:1489–504.
- Unger MS, Li E, Scharnagl L, Poupardin R, Altendorfer B, Mrowetz H, Hutter-Paier B, Weiger TM, Heneka MT, Attems J, Aigner L. CD8(+) T-cells infiltrate Alzheimer's disease brains and regulate neuronal- and synapse-related gene expression in APP-PS1 transgenic mice. *Brain Behav Immun*. 2020;89:67–86.
- Gate D, Saligrama N, Leventhal O, Yang AC, Unger MS, Middeldorp J, Chen K, Lehallier B, Channappa D, De Los Santos MB, et al. Clonally expanded CD8 T cells patrol the cerebrospinal fluid in Alzheimer's disease. *Nature*. 2020;577:399–404.
- Merlini M, Kirabali T, Kulic L, Nitsch RM, Ferretti MT. Extravascular CD3+ T cells in brains of alzheimer disease patients correlate with tau but not with amyloid pathology: an immunohistochemical study. *Neurodegener Dis*. 2018;18:49–56.
- Derk J, Jones HE, Como C, Pawlikowski B, Siegenthaler JA. Living on the edge of the CNS: meninges cell diversity in health and disease. *Front Cell Neurosci*. 2021;15: 703944.
- Rua R, McGavern DB. Advances in meningeal immunity. *Trends Mol Med*. 2018;24:542–59.
- Zhang Y, Bailey JT, Xu E, Singh K, Lavaert M, Link VM, D'Souza S, Hafiz A, Cao J, Cao G, et al. Mucosal-associated invariant T cells restrict reactive oxidative damage and preserve meningeal barrier integrity and cognitive function. *Nat Immunol*. 2022;23:1714–25.
- Ye L, Pan J, Pasha MA, Shen X, D'Souza SS, Fung ITH, Wang Y, Guo B, Tang DD, Yang Q. Mucosal-associated invariant T cells restrict allergic airway inflammation. *J Allergy Clin Immunol*. 2020;145(1469–1473): e1464.
- Corbett AJ, Eckle SB, Birkinshaw RW, Liu L, Patel O, Mahony J, Chen Z, Reantragoon R, Meehan B, Cao H, et al. T-cell activation by transitory neo-antigens derived from distinct microbial pathways. *Nature*. 2014;509:361–5.
- Fung ITH, Sankar P, Zhang Y, Robison LS, Zhao X, D'Souza SS, Salinero AE, Wang Y, Qian J, Kuentzel ML, et al. Activation of group 2 innate lymphoid cells alleviates aging-associated cognitive decline. *J Exp Med*. 2020. <https://doi.org/10.1084/jem.20190915>.
- Zhang Y, Fung ITH, Sankar P, Chen X, Robison LS, Ye L, D'Souza SS, Salinero AE, Kuentzel ML, Chittur SV, et al. Depletion of NK cells improves cognitive function in the Alzheimer disease mouse model. *J Immunol*. 2020;205:502–10.
- Fung ITH, Zhang Y, Shin DS, Sankar P, Sun X, D'Souza SS, Song R, Kuentzel ML, Chittur SV, Zuloaga KL, Yang Q. Group 2 innate lymphoid cells are numerically and functionally deficient in the triple transgenic mouse model of Alzheimer's disease. *J Neuroinflammation*. 2021;18:152.

21. Yang Q, Monticelli LA, Saenz SA, Chi AW, Sonnenberg GF, Tang J, De Obaldia ME, Bailis W, Bryson JL, Toscano K, et al. T cell factor 1 is required for group 2 innate lymphoid cell generation. *Immunity*. 2013;38:694–704.
22. D'Souza SS, Shen X, Fung ITH, Ye L, Kuentzel M, Chittur SV, Furuya Y, Siebel CW, Maillard IP, Metzger DW, Yang Q. Compartmentalized effects of aging on group 2 innate lymphoid cell development and function. *Aging Cell*. 2019;18: e13019.
23. Ye L, Pan J, Liang M, Pasha MA, Shen X, D'Souza SS, Fung ITH, Wang Y, Patel G, Tang DD, Yang Q. A critical role for c-Myc in group 2 innate lymphoid cell activation. *Allergy*. 2020;75:841–52.
24. Lehmann JS, Zhao A, Sun B, Jiang W, Ji S. Multiplex cytokine profiling of stimulated mouse splenocytes using a cytometric bead-based immunoassay platform. *J Vis Exp*. 2017;129:56440.
25. Constantinides MG, Link VM, Tamoutounour S, Wong AC, Perez-Chaparro PJ, Han SJ, Chen YE, Li K, Farhat S, Weckel A, et al. MAIT cells are imprinted by the microbiota in early life and promote tissue repair. *Science*. 2019. <https://doi.org/10.1126/science.aax6624>.
26. Despres C, Byrne C, Qi H, Cantrelle FX, Huvent I, Chambraud B, Baulieu EE, Jacquot Y, Landrieu I, Lippens G, Smet-Nocca C. Identification of the Tau phosphorylation pattern that drives its aggregation. *Proc Natl Acad Sci U S A*. 2017;114:9080–5.
27. Goedert M, Jakes R, Vanmechelen E. Monoclonal antibody AT8 recognises tau protein phosphorylated at both serine 202 and threonine 205. *Neurosci Lett*. 1995;189:167–9.
28. Mancuso R, Fryatt G, Cleal M, Obst J, Pipi E, Monzon-Sandoval J, Ribe E, Winchester L, Webber C, Nevado A, et al. CSF1R inhibitor JNJ-40346527 attenuates microglial proliferation and neurodegeneration in P301S mice. *Brain*. 2019;142:3243–64.
29. Wang C, Fan L, Khawaja RR, Liu B, Zhan L, Kodama L, Chin M, Li Y, Le D, Zhou Y, et al. Microglial NF-kappaB drives tau spreading and toxicity in a mouse model of tauopathy. *Nat Commun*. 1969;2022:13.
30. Gratuze M, Schlachetzki JCM, D'Oliveira Albanus R, Jain N, Novotny B, Brase L, Rodriguez L, Mansel C, Kipnis M, O'Brien S, et al. TREM2-independent microgliosis promotes tau-mediated neurodegeneration in the presence of ApoE4. *Neuron*. 2023;111(202–219): e207.
31. Mathys H, Davila-Velderrain J, Peng Z, Gao F, Mohammadi S, Young JZ, Menon M, He L, Abdurrob F, Jiang X, et al. Single-cell transcriptomic analysis of Alzheimer's disease. *Nature*. 2019;570:332–7.
32. Koay HF, Su S, Amann-Zalcenstein D, Daley SR, Comerford I, Miosge L, Whyte CE, Konstantinov IE, d'Udekem Y, Baldwin T, et al. A divergent transcriptional landscape underpins the development and functional branching of MAIT cells. *Sci Immunol*. 2019. <https://doi.org/10.1126/sciimmunol.aay6039>.
33. Godfrey DI, Koay HF, McCluskey J, Gherardin NA. The biology and functional importance of MAIT cells. *Nat Immunol*. 2019;20:1110–28.
34. Huang S, Gilfillan S, Cella M, Miley MJ, Lantz O, Lybarger L, Fremont DH, Hansen TH. Evidence for MR1 antigen presentation to mucosal-associated invariant T cells. *J Biol Chem*. 2005;280:21183–93.
35. Patel O, Kjer-Nielsen L, Le Nours J, Eckle SB, Birkinshaw R, Beddoe T, Corbett AJ, Liu L, Miles JJ, Meehan B, et al. Recognition of vitamin B metabolites by mucosal-associated invariant T cells. *Nat Commun*. 2013;4:2142.
36. Gherardin NA, Keller AN, Woolley RE, Le Nours J, Ritchie DS, Neeson PJ, Birkinshaw RW, Eckle SBG, Waddington JN, Liu L, et al. Diversity of T cells restricted by the MHC Class I-related molecule MR1 facilitates differential antigen recognition. *Immunity*. 2016;44:32–45.
37. Edmans MD, Connelley TK, Morgan S, Pediongco TJ, Jayaraman S, Juno JA, Meehan BS, Dewar PM, Maze EA, Roos EO, et al. MAIT cell-MR1 reactivity is highly conserved across multiple divergent species. *J Biol Chem*. 2024;300: 107338.
38. Legoux F, Bellet D, Daviaud C, El Morr Y, Darbois A, Niort K, Procopio E, Salou M, Gilet J, Ryffel B, et al. Microbial metabolites control the thymic development of mucosal-associated invariant T cells. *Science*. 2019;366:494–9.
39. Andriova H, Miltiadous O, Kousa AI, Dai A, DeWolf S, Violante S, Park HY, Janaki-Raman S, Gardner R, El Daker S, et al. MAIT and Vdelta2 unconventional T cells are supported by a diverse intestinal microbiome and correlate with favorable patient outcome after allogeneic HCT. *Sci Transl Med*. 2022. <https://doi.org/10.1126/scitranslmed.abj2829>.
40. Jabeen MF, Hinks TSC. MAIT cells and the microbiome. *Front Immunol*. 2023;14:1127588.
41. Marsh SE, Walker AJ, Kamath T, Dissing-Olesen L, Hammond TR, de Soysa TY, Young AMH, Murphy S, Abdurouf A, Nadaf N, et al. Dissection of artifactual and confounding glial signatures by single-cell sequencing of mouse and human brain. *Nat Neurosci*. 2022;25:306–16.
42. Wyatt-Johnson SK, Kersey HN, Codocedo JF, Newell KL, Landreth GE, Lamb BT, Oblak AL, Brutkiewicz RR. Control of the temporal development of Alzheimer's disease pathology by the MR1/MAIT cell axis. *J Neuroinflammation*. 2023;20:78.

Publisher's Note

Springer Nature remains neutral with regard to jurisdictional claims in published maps and institutional affiliations.